IOP Publishing Phys. Scr. 99 (2024) 065263 https://doi.org/10.1088/1402-4896/ad4b62

Physica Scripta

RECEIVED
26 December 2023

REVISED
21 April 2024

ACCEPTED FOR PUBLICATION
14 May 2024

PUBLISHED
24 May 2024

PAPER

Fusion and fission phenomena in a (2+1)-dimensional Sawada-Kotera type system

Jianyong Wang[1], **Yunqing Yang**[2], **Xiaoyan Tang**[3] and **Yong Chen**[1,3]

[1] Department of Mathematics and Physics, Quzhou University, Quzhou 324000, People's Republic of China
[2] School of Science, Zhejiang University of Science and Technology, Hangzhou, 310023, People's Republic of China
[3] School of Mathematical Sciences, Key Laboratory of Mathematics and Engineering Applications(Ministry of Education) & Shanghai Key Laboratory of PMMP, East China Normal University, Shanghai 200241, People's Republic of China

E-mail: jywangqz@126.com

Keywords: (2+1)-dimensional Sawada-Kotera type system, Localized excitation, Semi-rational solution, Generalized multilinear variable separation approach

Abstract

In this study, we extend the generalized multilinear variable separation approach to a fifth-order nonlinear evolution equation. By performing asymptotic analysis on the variable separation solution, which is composed of three lower-dimensional functions, we identify a resonant regime governing dromion-dromion/solitoff interactions. In the case of two-dromion interactions, elastic, inelastic, and completely inelastic collisions are possible, while for the dromion-solitoff interaction only inelastic and completely inelastic collisions are permitted. Furthermore, we derive two types of semi-rational solutions from the quadratic function ansatz. In particular, in the scenario of a completely resonant collision between a lump and a line-soliton pair, the lump separates from one line soliton and exists briefly before merging with the other soliton, forming a localized lump in both time and space dimensions. The fusion or fission phenomena between the dromion-dromion/solitoff interaction and the lump-line soliton interaction are shown graphically.

1. Introduction

Solitons, characterized as coherent and robust solitary wave solutions of nonlinear partial differential equations (NPDEs), have attracted considerable interest in various branches of physics due to their particle-like properties [1]. The exploration of multi-soliton solutions for a specific class of NPDEs, referred to as integrable systems or soliton equations, has been the focus of extensive research. Various effective methods have been developed for this purpose, including the inverse scattering method [2], Bäcklund and Darboux transformations [3, 4], the Hirota bilinear method [5], Riemann-Hilbert method [6–8], and the similarity transformation [9].

The separation of variables, one of the oldest methods in mathematical physics, has been effectively extended to its nonlinear counterpart from various perspectives. Examples of these extensions include the nonlinearization of the Lax pair [10], the symmetry constraint method [11], the multilinear variable separation approach (MLVSA) and the generalized MLVSA [12–14]. Among these methods, the MLVSA and its generalization are critical and powerful tools for obtaining localized excitations in numerous (2+1)-dimensional integrable systems [15–19]. Mathematically, there exists a universal formula for all MLVSA solvable systems, such as the Davey-Stewartson equation [15], the Broer-Kaup-Kupershmidt system [17], the (2+1)-dimensional sine-Gordon system [18], and the non-integrable (2+1)-dimensional Korteweg–de Vries equation [19]. Notably, new patterns of localized excitations, such as ring solitons, peakons, compactons, as well as chaotic and fractal patterns, have been constructed based on the universal formula. Although the MLVSA is initially proposed for (2+1)-dimensional systems, it can also be employed to solve (1+1)-dimensional [20] and (3+1)-dimensional [21] nonlinear systems.

Unlike solitons, which are localized in a specific direction, lumps represent rational solutions localized in all spatial directions [22]. Notably, lumps occur in various physical systems, including nonlinear fiber optics, plasmas, and Bose–Einstein condensates. Recent research demonstrates that the derivation of lump solutions is achievable through the quadratic functions ansatz, as illustrated by the Kadomtsev-Petviashvili (KP) equation [23–25]. Subsequently, these findings have prompted a comprehensive exploration of lump excitations and interaction solutions between lumps and other types of nonlinear waves [26–30]. For example, Hossen obtained three types of interaction solutions to a (3+1)-dimensional model, including the lump-kink wave solution, breathers, and a new interaction solution among the lumps, kink waves and periodic waves [29]. Li constructed degenerate lump solutions for the Yu-Toda-Sasa-Fukuyama equation using Hirota's bilinear method and a novel limit approach [30]. Further study suggests that interactions between a lump and a line-soliton pair could lead to the creation of rogue waves [31, 32].

In this work, we deal with the following (2+1)-dimensional Sawada-Kotera (2DSK) type system [33]

$$\begin{aligned} &u_t + u_{xxxxx} + 5(uv_{xx} + 2u_{xx}v + 3uv^2)_x = 0,\\ &u_x - v_y = 0. \end{aligned} \tag{1}$$

It is obvious that setting $u = v = w(x, y, t)$ and rescaling $y \to x$ would degenerate the 2DSK type system (1) into the SK equation [34, 35]. The 2DSK system (1), as a (2+1)-dimensional extension of the SK equation, serves as a model for surface water waves and may have applications in conformal field theory, quantum gravity, and nematic liquid crystals [36, 37].

The paper is organized as follows. Section 2 introduces an extended variable separation solution and examines its intricate relationship with the universal formula obtained by the MLVSA. Sections 3 and 4 analyze the dromion-dromion/solitoff interaction, establishing parameter conditions for elastic, inelastic, and completely inelastic scenarios via asymptotic analysis. In section 5, specific solutions are derived through a combined application of the quadratic function ansatz and the Hirota bilinear method, with a particular emphasis on completely resonant collisions. The concluding section presents several key findings.

2. Variable seperation solution

To apply the generalized MLVSA [38], we take the truncated Laurent series

$$u = 2(\ln f)_{xy} + u_0, \qquad v = 2(\ln f)_{xx} + v_0, \tag{2}$$

where u_0 and v_0 are arbitrary seed solutions to the 2DSK system. By substituting the transformation (2) with a specific choice of seed solution $u_0 = 0$ and $v_0 = v_0(x, t)$ into (1), after integrating with respect to x, we obtain the following bilinear equation

$$[D_y D_x^5 + 10v_0 D_y D_x^3 + 5(v_{0xx} + 3v_0^2)D_y D_x + D_y D_t + C(y, t)]f \cdot f = 0, \tag{3}$$

where f is an analytic function of (x, y, t) and the Hirota bilinear derivative operator is defined by [39]

$$D_x^l D_y^m D_t^n a \cdot b = (\partial_x - \partial_{x'})^l (\partial_y - \partial_{y'})^m (\partial_t - \partial_{t'})^n a(x, y, t) b(x', y', t')|_{x=x', y=y', t=t'}.$$

To completely separate the spatial variables $\{x, y\}$, we assume the expansion of the function f in the form

$$f = p_1 + p_2 q, \tag{4}$$

where p_1 and p_2 are functions of $\{x, t\}$, and q is a function of $\{y, t\}$, respectively. Substituting (4) into (3) leads to

$$[D_t + D_x^5 + 10v_0 D_x^3 + 5(v_{0xx} + 3v_0^2)D_x]p_1 \cdot p_2 = \frac{p_2 q_{yt} f + 2C(y, t) f^2}{q_y} - p_2^2 q_t. \tag{5}$$

By introducing the restriction

$$C(y, t) = 2c_1 q_y, \tag{6}$$

equation (5) can be separated into the following two equations

$$[D_t + D_x^5 + 10v_0 D_x^3 + 5(v_{0xx} + 3v_0^2)D_x]p_1 \cdot p_2 = (c_1 p_1^2 + c_2 p_2^2 + c_3 p_1 p_2), \tag{7}$$

$$q_t = -c_1 q^2 + c_3 q - c_2, \tag{8}$$

where c_1, c_2 and c_3 are arbitrary functions of t. Now, the problem of finding the solution of f is transformed into a task of determining solutions for the reduced differential equations (7) and (8). Interestingly, the first-order differential equation (8) is known as the nonlinear Riccati equation, whose solution can be given explicitly

$$q = \frac{T_1}{T_3 + F} + T_2, \tag{9}$$

where $T_i = T_i(t)$, $(i = 1, 2, 3)$ and $F = F(y)$ are arbitrary functions of the indicated variables while c_0, c_1, and c_2 are related to T_1, T_2 and T_3 by

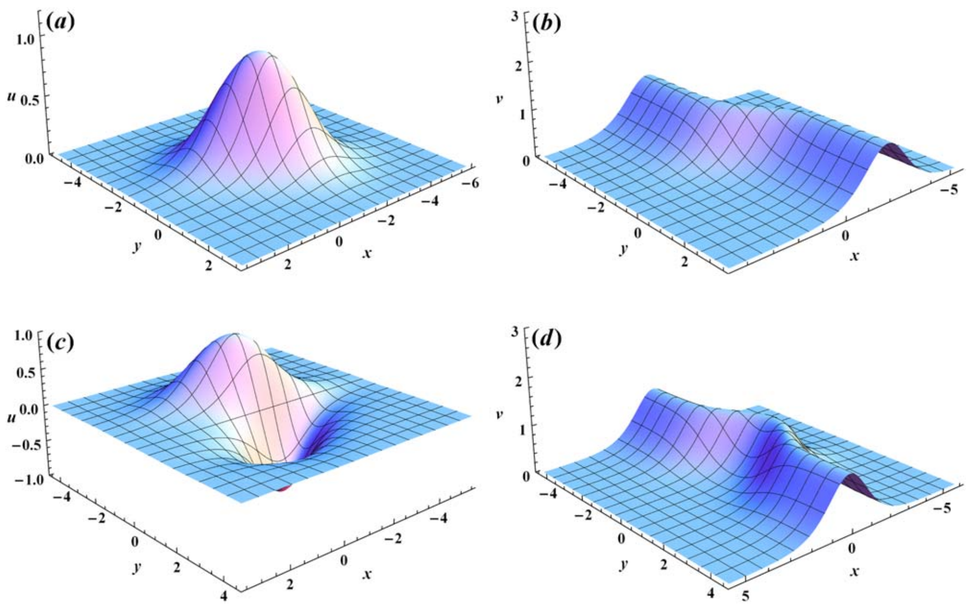

Figure 1. Plots of dromion structure and the corresponding v field with parameters are $k_1 = 1.5, l = 2, \alpha = \xi_{10} = 0$ and $K = 20$. (a) a standard dromion structure with $Y = e^{ly}$; (b) the corresponding v field; (c) a dipole dromion structure with $Y = \operatorname{sech}(ly)$; (d) the corresponding v field.

$$c_1(t) = \frac{T_{3t}}{T_1}, \quad c_2(t) = \frac{T_2 T_{1t}}{T_1} + \frac{T_2^2 T_{3t}}{T_1} - T_{2t}, \quad c_3(t) = 2\frac{T_2 T_{3t}}{T_1} + \frac{T_{1t}}{T_1}. \tag{10}$$

Finally, substituting (4) into (2) yields the variable separation solutions of the 2DSK system

$$u = -\frac{2(p_{1x}p_2 - p_1 p_{2x})q_y}{(p_1 + p_2 q)^2}, \quad v = \frac{2(p_{1xx} + p_{2xx}q)}{(p_1 + p_2 q)} - \frac{2(p_{1x}^2 + 2p_{1x}p_{2x}q - p_{2x}^2 q^2)}{(p_1 + p_2 q)^2} + v_0. \tag{11}$$

Given $p_1 = a_1 + a_3 p$ and $p_2 = a_0 + a_2 p$, we find that the field u takes the form of the universal formula for all MLVSA solvable systems

$$u = -\frac{2(a_0 a_3 - a_1 a_2)p_x q_y}{(a_0 + a_1 p + a_2 q + a_3 pq)^2},$$

where p is a function of $\{x, t\}$, and a_0, a_1, a_2, a_3 are constants.

3. Elastic, inelastic and completely inelastic interaction between two dromions

3.1. Dynamic characteristics of a single dromion structure

The exponentially localized dromion structure is an important nonlinear excitation in high dimensions [40–45]. It appears in various physical systems, such as the magnetosphere of Saturn [44] and the disk-shaped dipolar Bose–Einstein condensate [45].

To construct the dromion structure for the u field, we set $T_1 = 1, T_2 = T_3 = 0$, indicating $q = Y = Y(y)$, and $v_0 = \alpha$ as a constant. Subsequently, equations (7)–(8) can be satisfied by taking

$$p_1 = 1 + e^{\xi_1}, \quad p_2 = 1 + Ke^{\xi_1}, \quad \xi_1 = k_1 x + \omega_1 t + \xi_{10}, \quad \omega_1 = -k_1^5 - 10\alpha k_1^3 - 15\alpha k_1. \tag{12}$$

With the additional restriction $Y = e^{\eta}$, where $\eta = ly$, the substitution of (12) into equation (11) yields

$$u = \frac{2k_1 l(K-1)e^{\xi_1+\eta}}{(1 + e^{\xi_1} + e^{\eta} + Ke^{\xi_1+\eta})^2}, \quad v = \frac{2k_1^2 e^{\xi_1}(1 + e^{\eta})(1 + Ke^{\eta})}{(1 + e^{\xi_1} + e^{\eta} + Ke^{\xi_1+\eta})^2}. \tag{13}$$

Here, the u field illustrates a single dromion structure, as depicted in figures 1(a), while the v field represents a line soliton with a sudden shift, as shown in figures 1(b). Setting $Y = \operatorname{sech}(2y)$, a dipole dromion, which is a bounded state of a bright and a dark dromion, is observed in figures 1(c). For the corresponding v field, a line soliton with a bump is evident in figures 1(d).

To characterize the single dromion structure, its amplitude and mass can be defined [43]. By setting the partial derivatives u_x and u_y to zero, it is found that the tip of the dromion is located at the critical point where $e^{\eta_1} = e^{\eta_2} = \frac{1}{\sqrt{K}}$, resulting in the amplitude

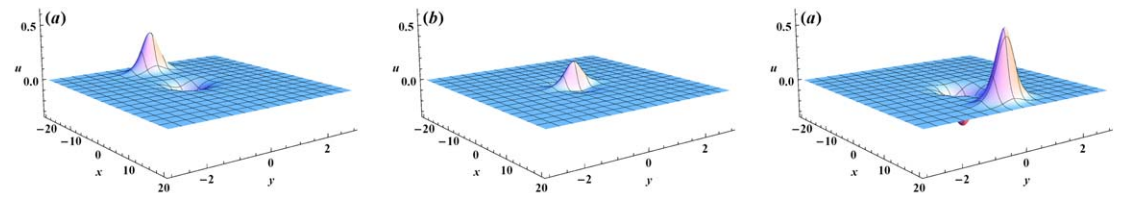

Figure 2. Inelastic interaction between bright-dark dromions with parameters $k_1 = 0.8, k_2 = 1.25, l = 5, K_1 = 0.9, K_2 = 0.5, K_3 = 1.6$ and $\xi_{10} = \xi_{20} = \alpha = 0$. (a) $t = -6$; (b) $t = 0$; (c) $t = 6$.

$$u_{\max} = \frac{1}{2}\frac{|k_1 l|(K-1)}{(\sqrt{K}+1)^2}. \tag{14}$$

The mass of the single dromion is defined as

$$M = \int_{-\infty}^{+\infty}\int_{-\infty}^{+\infty} u dxdy = 2\ln(K). \tag{15}$$

3.2. Elastic, inelastic and completely inelastic interaction

In addition to equation (12), one may take

$$p_1 = 1 + e^{\xi_1} + e^{\xi_2} + K_1 e^{\xi_1+\xi_2}, \quad p_2 = 1 + K_2 e^{\xi_1} + K_3 e^{\xi_2} + K e^{\xi_1+\xi_2}, \quad \xi_i = k_i x + \omega_i t + \xi_{i0}, \quad (i = 1, 2) \tag{16}$$

to produce a two-dromion solution. Substituting (16) into (7), the coefficient K and the dispersion relation can be determined as

$$K = K_1 + \frac{(k_1 - k_2)(k_1^2 - k_1 k_2 + k_2^2 + 6\alpha)}{(k_1 + k_2)(k_1^2 + k_1 k_2 + k_2^2 + 6\alpha)}(K_2 - K_3), \quad \omega_i = -k_i^5 - 10\alpha k_i^3 - 15\alpha k_i, \quad (i = 1, 2). \tag{17}$$

To carry out the asymptotic analysis of the interaction between two dromions, without loss of generality, we assume $k_1 > 0, k_2 > 0, \omega_1/k_1 > \omega_2/k_2$ and e^{η} is finite. In the frame comoving with ξ_1, the exponent ξ_1 is finite, and the limits $t \to \pm\infty$ leads to

$$u_{1b} = \frac{2k_1 l(K - K_1K_3)e^{\xi_1+\eta}}{(1 + K_1 e^{\xi_1} + K_3 e^{\eta} + K e^{\xi_1+\eta})^2} \quad t \to -\infty; \quad u_{1a} = \frac{2k_1 l(K_2 - 1)e^{\xi_1+\eta}}{(1 + e^{\xi_1} + e^{\eta} + K_2 e^{\xi_1+\eta})^2}, \quad t \to +\infty, \tag{18}$$

where u_{1b} and u_{1a} stand for the expression of dromion 1 before and after the interaction, respectively. Analogously, the expressions for dromion 2 before and after the interaction are

$$u_{2b} = \frac{2k_2 l(K_3 - 1)e^{\xi_2+\eta}}{(1 + e^{\xi_2} + e^{\eta} + K_3 e^{\xi_2+\eta})^2}, \quad t \to -\infty; \quad u_{2a} = \frac{2k_2 l(K - K_1K_2)e^{\xi_2+\eta}}{(1 + K_1 e^{\xi_1} + K_3 e^{\eta} + K e^{\xi_1+\eta})^2}, \quad t \to +\infty. \tag{19}$$

In general, the interaction between two dromions is remarkably inelastic. Nonetheless, if the additional conditions $u_{1b}(\xi_1 + \delta_{1x}, \eta + \delta_{1y}) = u_{1a}(\xi_1, \eta)$ and $u_{2b}(\xi_2 + \delta_{2x}, \eta + \delta_{2y}) = u_{2a}(\xi_2, \eta)$ are imposed, namely,

$$K = K_1K_2K_3, \quad K_1 = \frac{(k_1 - k_2)(k_1^2 - k_1k_2 + k_2^2)(K_2 - K_3)}{(k_1 + k_2)(k_1^2 + k_1k_2 + k_2^2)(K_2K_3 - 1)}, \quad (K_2 \neq K_3), \tag{20}$$

then the interaction between two dromions becomes elastic and the phase shifts can be determined as

$$\delta_{1x} = -\ln(K_1), \quad \delta_{1y} = -\ln(K_3), \quad \delta_{2x} = \ln(K_1), \quad \delta_{2y} = \ln(K_2). \tag{21}$$

Figure 2 illustrates the inelastic interaction between bright-dark dromions, showing obvious shape changes and phase shifts in the transverse direction. An elastic interaction is presented in figure 3, plotting the quantity '$-u$', where the two dark dromions maintain their identity after the interaction, except for phase shifts. Interestingly, a completely inelastic interaction between two dromions, namely, fusion or fission phenomena, can be observed by imposing the additional condition $K = K_1K_2$ or $K = K_1K_3$. A schematic diagram depicting the fission process of bright dromions with $K_1 = K/K_2 \simeq 26.27$ is shown in figure 4.

According to the definition (15), the total mass of two dromions before and after the interaction can be calculated as follows

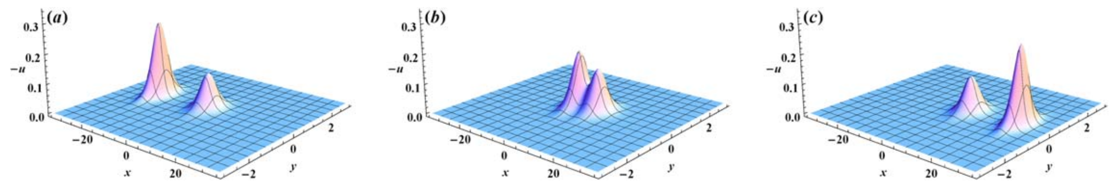

Figure 3. Elastic interaction between two dark dromions with parameters are $k_1 = 0.9, k_2 = 0.65, l = -5, K_2 = 1.6, K_3 = 1.35$ and $\xi_{10} = \xi_{20} = \alpha = 0$. (a) $t = -30$; (b) $t = -0$; (c) $t = 30$.

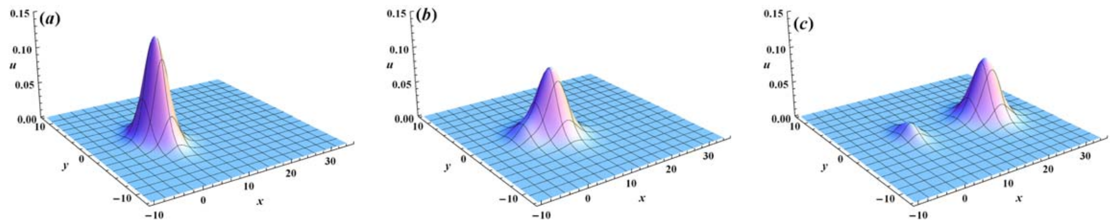

Figure 4. Completely inelastic interaction between two bright dromions: the fission process, characterized by the parameters are $k_1 = -0.9, k_2 = 0.6, l = -1, K_2 = 1.2, K_3 = 0.3, \xi_{10} = \xi_{20} = 0$ and $\alpha = -0.5$. (a) $t = 0$; (b) $t = 3$; (c) $t = 10$.

$$\int_{-\infty}^{+\infty}\int_{-\infty}^{+\infty}(u_{1b} + u_{2b})dxdy = \int_{-\infty}^{+\infty}\int_{-\infty}^{+\infty}(u_{1a} + u_{2a})dxdy = 2\ln\left(\frac{K}{K_1}\right). \tag{22}$$

This proves that the total mass of two dromions is a conserved quantity, regardless of whether the interaction is elastic or not.

4. Inelastic and completely inelastic interaction between a solitoff and a dromion

For further simplicity, we set $T_1 = 1, T_2 = T_3 = 0$, and $v_0 = 0$. Then, equations (7)–(8) can be satisfied by taking

$$\begin{aligned} &p_1 = 1 + A_1e^{\xi_1} + A_2e^{\xi_2} + A_3e^{\xi_1+\xi_2}, \quad p_2 = B_0 + B_1e^{\xi_1} + B_2e^{\xi_2} + B_3e^{\xi_1+\xi_2}, \quad q = e^{\eta},\\ &\xi_1 = k_1x + \omega_1t + \xi_{10}, \quad \xi_2 = k_2x + \omega_2t + \xi_{20}, \quad \eta = ly, \quad \omega_1 = -k_1^5, \quad \omega_2 = -k_2^5, \end{aligned} \tag{23}$$

with coefficients A_i and B_j satisfy

$$(k_1 - k_2)(k_1^2 - k_1k_2 + k_2^2)(A_1B_2 - A_2B_1) + (k_1 + k_2)(k_1^2 + k_1k_2 + k_2^2)(B_3 - A_3B_0) = 0. \tag{24}$$

To interpret the interaction behavior clearly, we carry out the asymptotic analysis as in section 3. Without loss of generality, we assume $k_2 > k_1 > 0$ and e^{η} is finite. In the frame comoving with ξ_1, the limits $t \to \pm\infty$ leads to

$$u_{1b} = \frac{2k_1l(A_2B_3 - A_3B_2)e^{\xi_1+\eta}}{(A_2 + A_3e^{\xi_1} + B_2e^{\eta} + B_3e^{\xi_1+\eta})^2} \quad t \to -\infty; \quad u_{1a} = \frac{2k_1l(B_1 - A_1B_0)e^{\xi_1+\eta}}{(1 + A_1e^{\xi_1} + B_0e^{\eta} + B_1e^{\xi_1+\eta})^2} \quad t \to +\infty, \tag{25}$$

Analogously, in the frame comoving with ξ_2, the limits $t \to \pm\infty$ leads to

$$u_{2b} = \frac{2k_2l_3(B_2 - A_2B_0)e^{\xi_2+\eta}}{(1 + A_2e^{\xi_2} + B_0e^{\eta} + B_2e^{\xi_2+\eta})^2} \quad t \to -\infty; \quad u_{2a} = \frac{2k_2l(A_1B_3 - A_3B_1)e^{\xi_2+\eta}}{(A_1 + A_3e^{\xi_2} + B_1e^{\eta} + B_3e^{\xi_2+\eta})^2} \quad t \to +\infty. \tag{26}$$

From equations (25)–(26), it is clear that setting A_3 to zero, while keeping the other coefficients nonzero, can lead to an inelastic interaction between a soliton and a dromion. Furthermore, it can be inferred that the two waves exchange both energy and velocity during the interaction process. The amplitude changes can be summarized as follows:

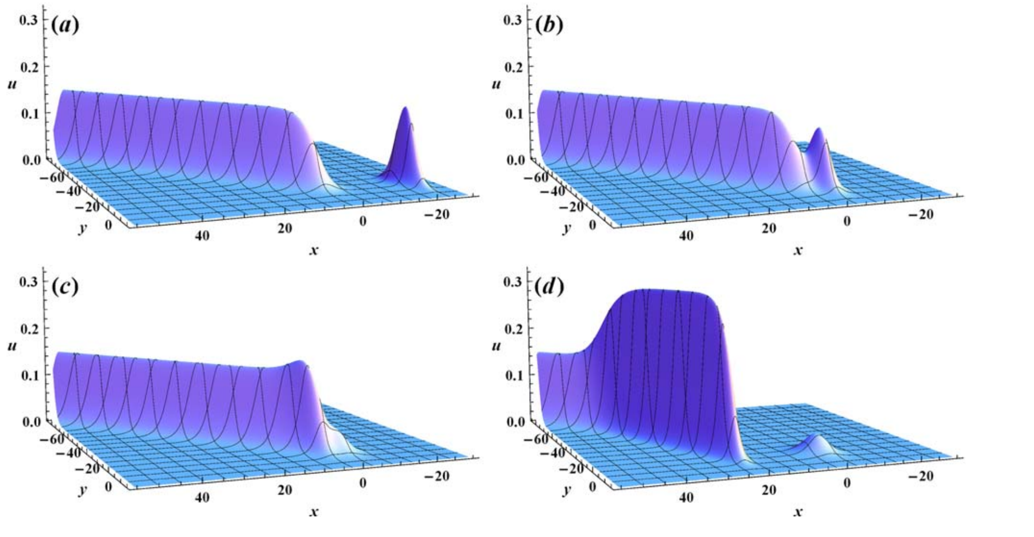

Figure 5. Inelastic interaction process between a solitoff and a dromion in the u field. (a) $t = -10$; (b) $t = -0.5$; (c) $t = 1$; (d) $t = 10$.

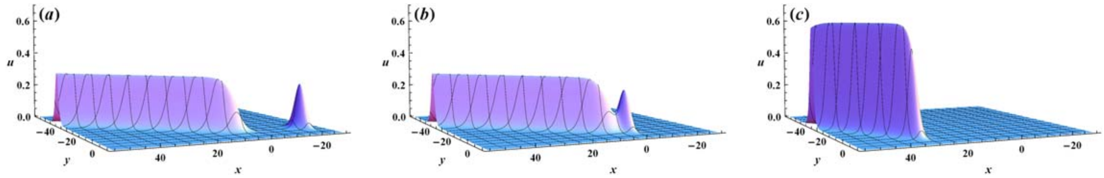

Figure 6. Completely inelastic collision between a solitoff and a dromion: fusion. A dromion is absorbed by a solitoff with parameters are $k_1 = 0.6, k_2 = 1.2, l = 1, A_2 = 2, A_3 = 0, B_0 = 1, B_2 = 12, B_3 = 1, \xi_{10} = \xi_{20} = \eta_0 = 0$ and $A_1 = B_1 = 0.7$. (a) $t = -10$; (b) $t = 0$; (c) $t = 15$;.

$$
\begin{aligned}
&A_{solitoff}|_{t\to-\infty} = A_{u_{1b}} = \frac{|k_1 l|}{2}, \quad A_{solitoff}|_{t\to+\infty} = A_{u_{2a}} = \frac{|k_2 l|}{2},\\
&A_{dromion}|_{t\to-\infty} = A_{u_{2b}} = \frac{|k_2 l(B_2 - A_2B_0)|M_-}{4A_2 + 2(B_2 + A_2B_0)M_-}, \quad M_- = \sqrt{\frac{A_2}{B_0B_2}}\\
&A_{dromion}|_{t\to+\infty} = A_{u_{1a}} = \frac{|k_1 l(B_1 - A_1B_0)|M_+}{4A_1 + 2(B_1 + A_1B_0)M_+}, \quad M_+ = \sqrt{\frac{A_1}{B_0B_1}}.
\end{aligned} \tag{27}
$$

Figure 5 illustrates an inelastic interaction process between a solitoff and a dromion. The parameters for this process include $k_1 = 0.6, k_2 = 1.2, l = 0.5, A_2 = 2, A_3 = 0, B_0 = 1, B_1 = 6, B_2 = 18, B_3 = 4, \xi_{10} = \xi_{20} = \eta_0 = 0$, and $A_1 = 20/9$. Figures 5 (a) shows that the two waves share the same initial amplitude $A_{u_{1b}} = A_{u_{2b}} = 0.15$. As the dromion's speed exceeds that of the solitoff, it will catch up with the solitoff and be slowed down due to its energy loss. As the dromion's bottom approaches the front of the solitoff, energy is transferred between them, causing the dromion's height to decrease. Comparing with figures 5(a), amplitude of the dromion structure decreases slightly, while no visible change of solitoff amplitude can be observed in figures 5(b). The accumulation of energy in the front part of the solitoff results in the formation of a hump on the peak, which is shown in figures 5(c). After the interaction process, significant changes in amplitude can be observed in both waves, as shown in figures 5(d).

Remarkably, completely inelastic interaction between a solitoff and a dromion become observable with the appropriate choice of wave parameters. By setting $B_1 - A_1B_0 = 0$, signifying the disappearance of the dromion, one can observe the absorption of a dromion structure by a solitoff, as depicted in figure 6. Similarly, one can observe the generation of a dromion from a solitoff, as shown in figure 7, by introducing the additional condtion $B_2 - A_2B_0 = 0$.

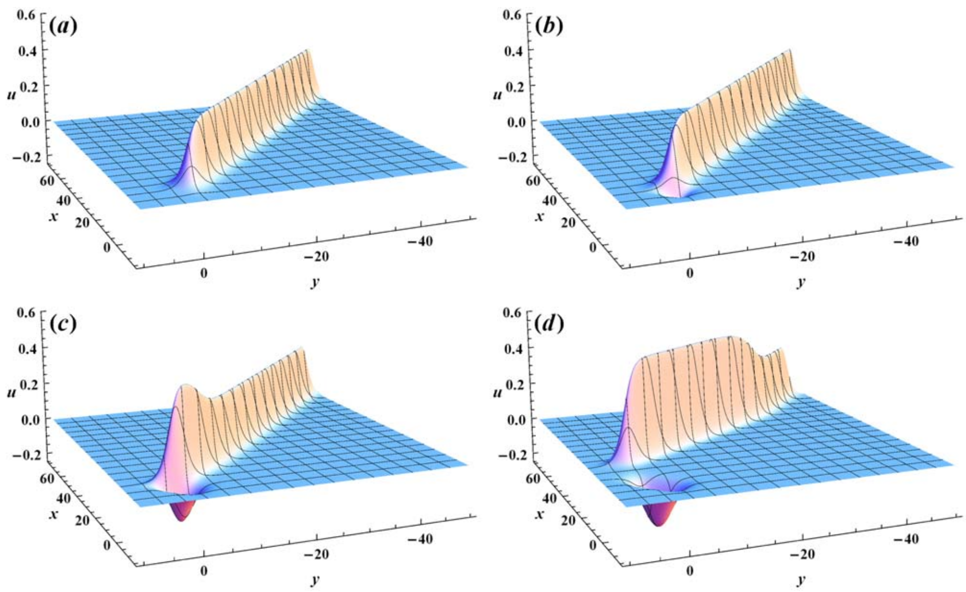

Figure 7. Completely inelastic collision between a solitoff and a dromion: fission. The emergence of a dromion from a solitoff with parameters are $k_1 = 0.6, k_2 = 1, l = 1, A_1 = 803/76, A_2 = 0.5, A_3 = 0, B_0 = 2, B_1 = 0.5, B_2 = B_3 = 1$, and $\xi_{10} = \xi_{20} = \eta_0 = 0$. (a) $t = -20$; (b) $t = -5$; (c) $t = 0$; (d) $t = 20$.

5. Interaction solutions between lump and line soliton

5.1. Lump solution

Take $C(y, t) = 0$ and v_0 as constant, the bilinear equation (3) reduce to

$$[D_y D_x^5 + 10v_0 D_y D_x^3 + 15v_0^2 D_y D_x + D_y D_t] f \cdot f = 0. \tag{28}$$

To construct lump solution of the 2DSK system (1), we assume the function f takes the following quadratic form

$$\begin{aligned} f &= g^2 + h^2 + a_9, \\ g &= a_1 x + a_2 y + a_3 t + a_4, \\ h &= a_5 x + a_6 y + a_7 t + a_8, \end{aligned} \tag{29}$$

with a_i ($i = 1, 2,...,9$) are the wave parameters to be determined. By substituting (29) into the bilinear equation (28) and setting the coefficients of the space-time variables x, y and t to zero, we obtain

$$a_1 = -\frac{a_3}{15v_0^2}, \quad a_2 = -\frac{a_6 a_7}{a_3}, \quad a_5 = -\frac{a_7}{15v_0^2}. \tag{30}$$

Obviously, the parameters $\{a_3, a_4, a_6, a_7, a_8, a_9\}$ are left as arbitrary and $\{a_1, a_5\}$ are relevant to the seed solution v_0. Together with the transformation (2), the explicit solution in rational form reads

$$\begin{aligned} u &= \frac{8a_6(a_3 h - a_7 g)(a_3 g + a_7 h)}{15a_3 v_0^2 (a_9 + g^2 + h^2)^2}, \\ v &= \frac{(a_3^2 - a_7^2)(h^2 - g^2) - 4a_3 a_7 gh + a_9(a_3^2 + a_7^2)}{225v_0^4 (a_9 + g^2 + h^2)^2} + v_0, \end{aligned} \tag{31}$$

where g and h are

$$\begin{aligned} g &= -\frac{a_3}{15v_0^2}x - \frac{a_6 a_7}{a_3}y + a_3 t + a_4, \\ h &= -\frac{a_7}{15v_0^2}x + a_6 y + a_7 t + a_8. \end{aligned}$$

To ensure that the solution (31) is rationally localized in all spatial directions, we impose the constraint condition $v_0 a_3 a_6 \neq 0$. At any fixed time t, the rational solutions approach zero as $x^2 + y^2$ tends to infinity. Thus, the solution (31) represents typical lump structures. In order to analyze the characteristics of lump motion, we consider the example of the u field. Setting $u_x = u_y = 0$ reveals that the extreme values are located at the four critical points

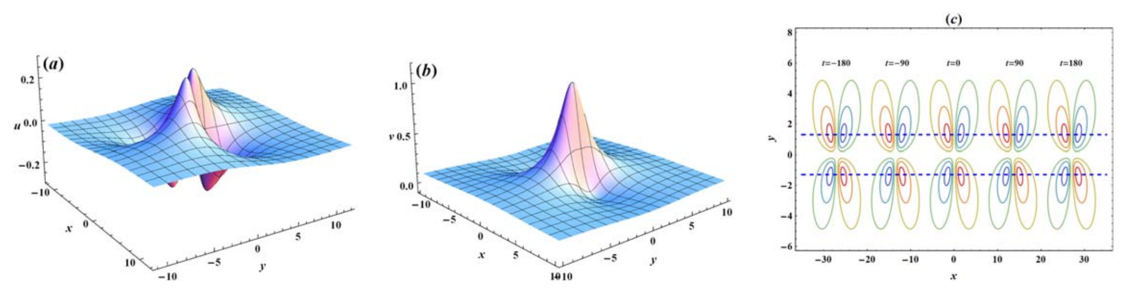

Figure 8. Plots of the lump structures of solution (31) with parameters are $a_3 = -0.12, a_4 = a_8 = 0, a_6 = 0.9, a_7 = 0.5$ and $a_9 = 50$, and $v_0 = 0.1$. (a) lump structure of u field; (b) lump structure of v field; (c) the contour plot of u in $x - y$ plane at different times.

$$\left[15v_0^2 t + \frac{30v_0^2(a_3a_4 + a_7a_8) \pm 15v_0^2\sqrt{2a_9(a_3^2 + a_7^2)}}{a_3^2 + a_7^2}, \frac{2a_3(a_4a_7 - a_3a_8) \pm a_3\sqrt{2a_9(a_3^2 + a_7^2)}\,]}{2a_6(a_3^2 + a_7^2)}\right], \tag{32}$$

which result in amplitude of u

$$u_{\max} = \left|\frac{a_6(a_3^2 + a_7^2)}{15v_0^2 a_3 a_9}\right|. \tag{33}$$

It is evident from equation (32) that the lump moves along the route line parallel to the x-axis with a velocity of $15v_0^2$. In order to provide a clearer visualization of the lump structure, let us examine some figures. Figures 8(a) exhibits the three-dimensional lump structure of u at time $t = 0$. According to equation (33), the amplitude of u can be approximately calculated as 0.26, consistent with the presented figure. Figures 8(b) displays the lump structure of v at time $t = 0$ on a constant background $v_0 = 0.1$. The contour maps at different times are shown in figures 8(c), where the trajectory of the lump's peak or valley is along the line $y = \pm 1.297$.

5.2. Lumpoff solution

The lumpoff solution describes completely inelastic interaction between lump waves and stripe line solitons[46]. It is characterized by the cutting of lump waves by soliton waves either before or after a specific time. To construct the lumpoff solution, we incorporate the exponential function into the quadratic function ansatz

$$\begin{aligned} f &= g^2 + h^2 + a_{10}e^{\xi} + a_9, \\ g &= a_1x + a_2y + a_3t + a_4, \\ h &= a_5x + a_6y + a_7t + a_8, \\ \xi &= k_1x + k_2y + k_3t, \end{aligned} \tag{34}$$

with a_i, k_i and ω are real parameters to be determined later. Substitution for (34) into the bilinear equation (28) yields, after elimination of the coefficients of polynomials x, y, and t, a set of more algebraic equations. From these equations, a nontrivial solution of five wave parameters $\{a_3, a_7, a_{10}, k_3, v_0\}$ can be determined as

$$a_3 = -\frac{5a_1k_1^4}{12}, \quad a_7 = -\frac{5a_5k_1^4}{12}, \quad a_{10} = \frac{2(a_1a_2 + a_5a_6)}{k_1k_2}, \quad k_3 = \frac{k_1^5}{4}, \quad v_0 = -\frac{k_1^2}{6}. \tag{35}$$

For the sake of nonsingularity, the expression of a_{10} leads to the constraint condition $k_1k_2(a_1a_2 + a_5a_6) > 0$. Via the transformation (2), the lumpoff solution of the 2DSK system (1) is obtained as follows

$$\begin{aligned} u = {} & \frac{4[(a_1a_2 - a_5a_6)(h^2 - g^2) - 2(a_1a_6 + a_2a_5)hg + (a_1a_2 + a_5a_6)(a_9 + a_{10}e^{\xi})]}{(g^2 + h^2 + a_{10}e^{\xi} + a_9)^2} \\ & + \frac{2a_{10}e^{\xi}[k_1k_2(g^2 + h^2 + a_9) - 2k_1(a_2g + a_6h) - 2k_2(a_1g + a_5h)]}{(g^2 + h^2 + a_{10}e^{\xi} + a_9)^2}, \end{aligned} \tag{36}$$

$$v = \frac{4[(a_1h - a_5g)^2 - (a_1g + a_5h)^2 + (a_1^2 + a_5^2)(a_9 + a_{10}e^{\xi})] + 2a_{10}e^{\xi}[k_1^2(g^2 + h^2 + a_9) - 4(a_1g + a_5h)]}{(g^2 + h^2 + a_{10}e^{\xi} + a_9)^2} + v_0, \tag{37}$$

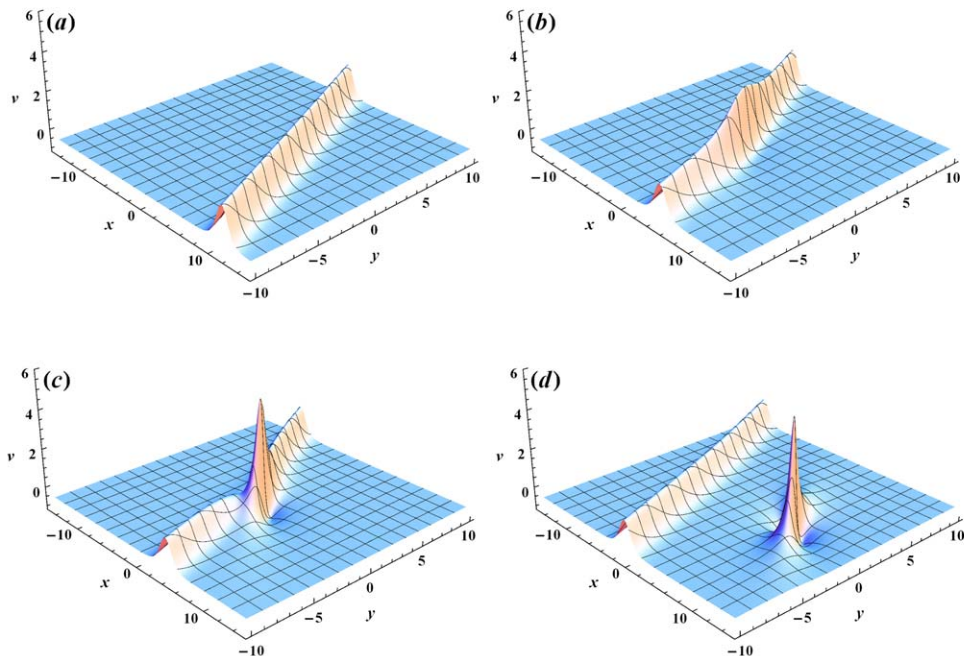

Figure 9. Time evolution of the lumpoff wave of the v field (37) with parameters are $a_1 = 1.05$, $a_2 = a_5 = 0.5$, $a_4 = a_8 = \xi_0 = v_0 = 0$, $a_5 = 0.5$, $a_6 = 1.5$, $a_9 = 1$, $k_1 = -1.8$ and $k_2 = -1.2$. (a) $t = -3$; (b) $t = -0.5$; (c) $t = 0$; (d) $t = 1.5$.

where g, h, and ξ are

$$\begin{aligned} g &= a_1 x + a_2 y - \frac{5a_1 k_1^4}{12} t + a_4, \\ h &= a_5 x + a_6 y - \frac{5a_5 k_1^4}{12} t + a_8, \\ \xi &= k_1 x + k_2 y + \frac{k_1^5}{4} t. \end{aligned} \tag{38}$$

The lumpoff solution (37) describes the completely inelastic interaction between a lump and a stripe soliton. Depending on the sign of k_3, it exhibits two notable nonlinear phenomena: fusion and fission. For illustration, we focus on the v component. It is assumed that x, y, and k_3 are constants, and $k_3 < 0$, without loss of generality. As $t \to -\infty$, the exponential term e^{ξ} primarily determines the solution, and v approaches v_0 as $\xi \to +\infty$. Therefore, there is no lump structure in this limit. In contrast, for $t \to +\infty$, the rational function $g^2 + h^2 + a_9$ dominates, implying that the lump structure tends to emerge and flourish. Based on these asymptotic analysis, it is obvious that the fission phenomenon may be observed by taking $k_3 < 0$ as shown in figure 9. At time of $t = -3$, only a line soliton moving towards the $-x$ direction is visible in figures 9 (a). In figures 9(b), the line soliton exhibits a slight curve, resulting in a hump at its center. In figures 9(c), one can observe that the line soliton has split into one lump structure and one line soliton at time $t = 0$. Figures 9(d) shows that the lump structure tends to depart from the soliton line as time goes on. Corresponding to this, figure 10 shows the contour plot. Furthermore, by taking $k_1 = 1.8$, and $k_2 = -1.2$ with other parameters unchanged one can observe the fusion process.

5.3. Instanton-like excitation

To explore a special instanton-like excitation generated by the resonant interaction between a lump a line-soliton pair, we assume

$$\begin{aligned} f &= g^2 + h^2 + a_{10} e^{\xi} + a_{11} e^{-\xi} + a_9, \\ g &= a_1 x + a_2 y + a_3 t + a_4, \\ h &= a_5 x + a_6 y + a_7 t + a_8, \\ \xi &= k_1 x + k_2 t, \end{aligned} \tag{39}$$

Substituting (39) into (28) and proceeding as previous section, we obtain a nontrivial solution of four determined wave parameters $\{a_1, a_5, a_{10}, a_{11}\}$

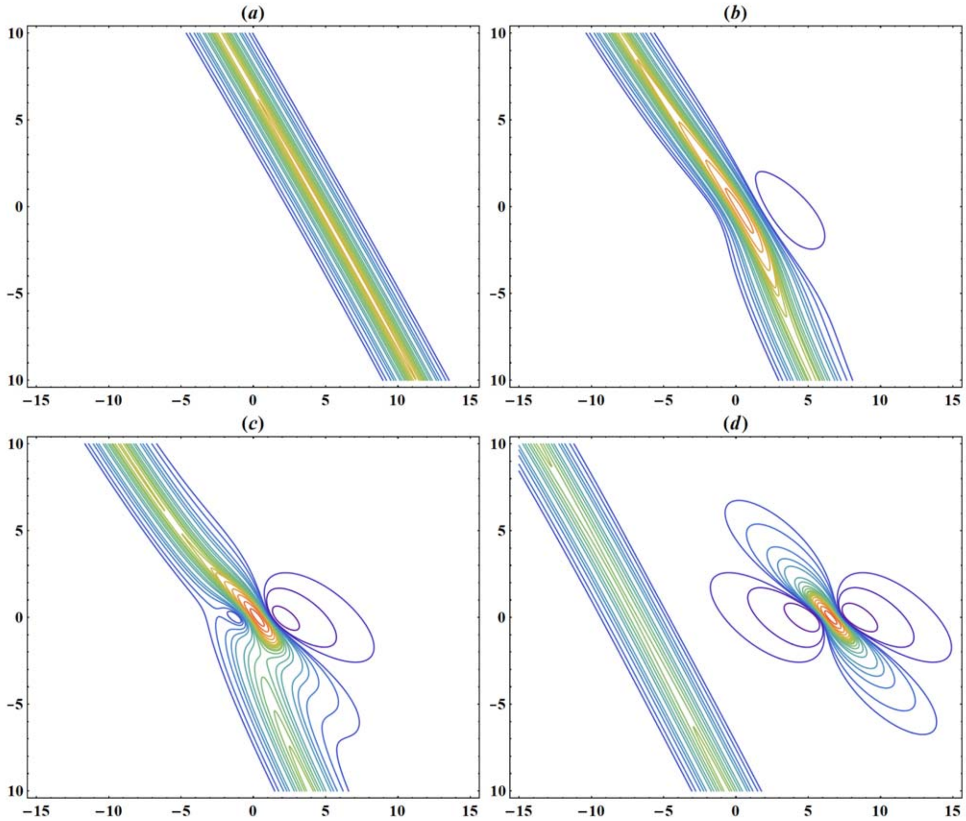

Figure 10. The corresponding contour plots of the lumpoff solution (37) at different times. (a) $t = -3$; (b) $t = -0.5$; (c) $t = 0$; (d) $t = 1.5$.

$$a_1 = -\frac{a_3}{15v_0^2},\quad a_5 = -\frac{a_7}{15v_0^2},\quad a_{10} = a_{11} = -\frac{2(a_3^2 + a_7^2)}{75k_1^2 v_0^3(6v_0 + k_1^2)}. \tag{40}$$

The expression of $\{a_i\}$ $(i = 1, 5, 10)$ leads to the constraint conditions: $v_0 k_1 \neq 0$, $v_0 < 0$ and $k_1^2 > 6|v_0|$. Through the transformation (2), the rational-exponential solution of the 2DSK system (1) reads

$$\begin{aligned} u &= \frac{4[(a_1a_2 - a_5a_6)(h^2 - g^2) - 2(a_1a_6 + a_2a_5)hg + (a_1a_2 + a_5a_6)(a_9 + a_{10}e^{\xi} + a_{11}e^{-\xi})]}{(g^2 + h^2 + a_{10}e^{\xi} + a_9)^2} \\ &- \frac{4a_{10}k_1(a_2g + a_6h)(e^{\xi} - e^{-\xi})}{(g^2 + h^2 + a_{10}e^{\xi} + a_9)^2}, \end{aligned} \tag{41}$$

$$\begin{aligned} v &= \frac{2a_{10}[k_1^2(g^2 + h^2 + a_9)(e^{\xi} + e^{-\xi}) - 4k_1(a_1g + a_5h)(e^{\xi} - e^{-\xi})]}{(g^2 + h^2 + a_{10}e^{\xi} + a_9)^2} \\ &+ \frac{4\{(a_1h - a_5g)^2 - (a_1g + a_5h)^2 + (a_1^2 + a_5^2)[a_9 + a_{10}(e^{\xi} + e^{-\xi})]\}}{(g^2 + h^2 + a_{10}e^{\xi} + a_9)^2} + v_0, \end{aligned} \tag{42}$$

where g, h, and ξ are

$$\begin{aligned} g &= -\frac{a_3}{15v_0^2}x + a_2y + a_3t + a_4, \\ h &= -\frac{a_7}{15v_0^2}x + a_6y + a_7t + a_8. \\ \xi &= k_1x + k_2t, \end{aligned} \tag{43}$$

The semi-rational solution (41)–(42) represents the completely inelastic interaction between a lump and a line-soliton pair. Since the exponential term is dominant, the lump wave rapidly vanishes as $t \to \pm\infty$. Therefore, the lump only becomes visible when it shifts to the line $\xi \to 0$. The asymptotic behavior of the solution (41)–(42) coincides with the concept of instanton in theoretical physics. Figure 11 illustrates such a phenomenon for the v component by means of three-dimensional plots and the corresponding contour plots are shown in figure 12. Graphically, the solution portrays the lump initially detaching from the line soliton, swiftly merging into the next adjacent soliton after a brief appearance on a constant background. This unique

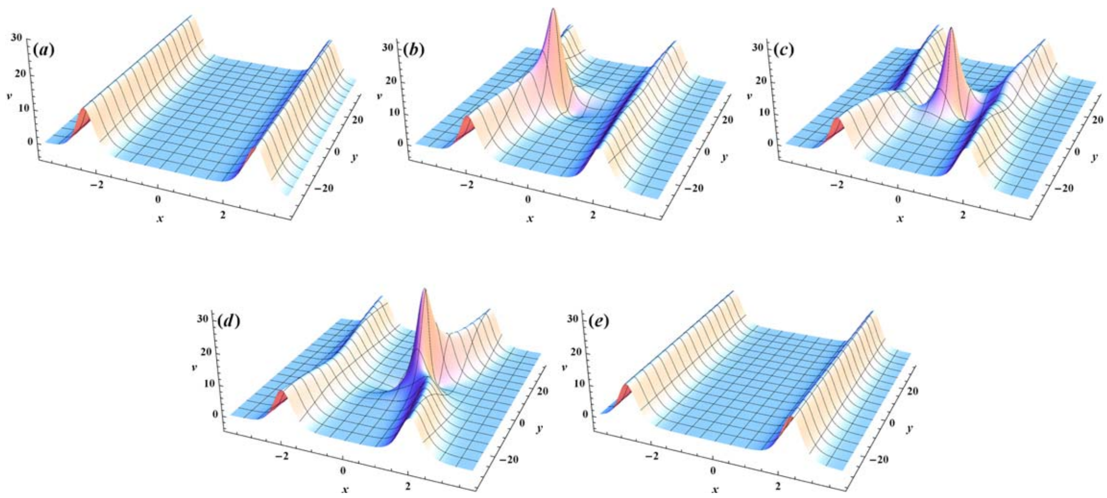

Figure 11. The three-dimensional plots of the rational-exponential solution of equation (42) at different times. The parameters are selected as $a_2 = 1.2, a_3 = 1.6, a_4 = a_8 = \xi_0 = 0, a_5 = 1, a_6 = 0.6, a_7 = -1.5, a_9 = 15, k_1 = 5, k_2 = 0.01, v_0 = -0.12$. (a) $t = -100$; (b) $t = -5$; (c) $t = 0$.(d) $t = 5$; (e) $t = 100$.

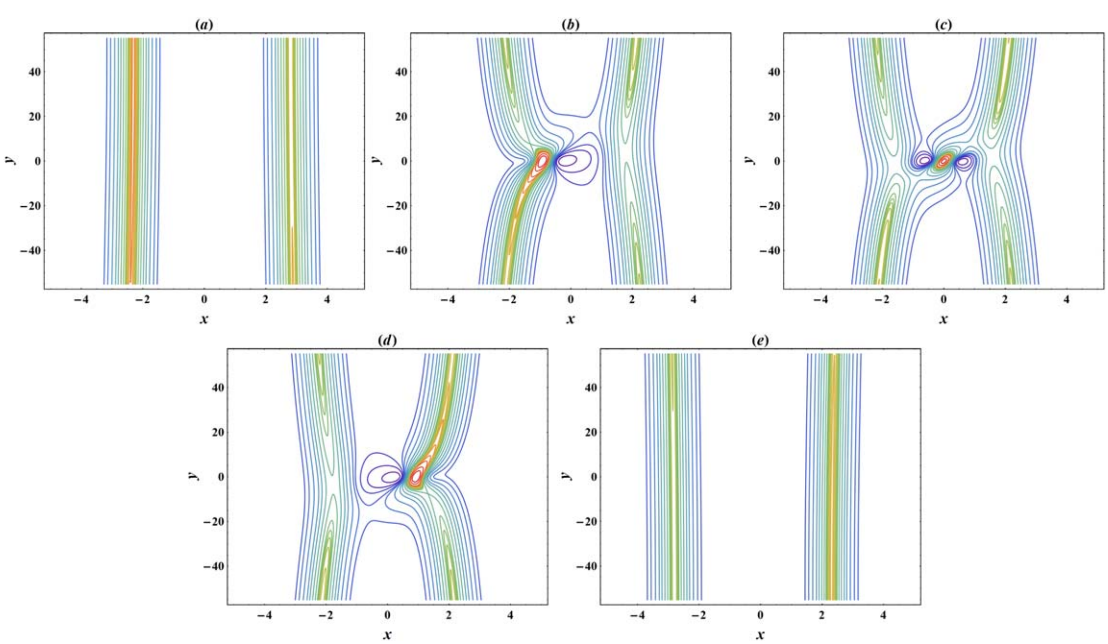

Figure 12. The corresponding contour plots of the rational-exponential solution of equation (42) at different times. (a) $t = -100$; (b) $t = -5$; (c) $t = 0$.(d) $t = 5$; (e) $t = 100$.

transient lump solution exhibits key characteristics of a two-dimensional rogue wave, displaying localization in both spatial and temporal dimensions, thus referred to as a rogue lump wave.

6. Conclusions and discussions

In this study, we have successfully extended the generalized MLVSA to a challenging fifth-order nonlinear evolution equation, specifically the 2DSK system. The solution of the variable separation is formulated in terms of three lower dimensional functions, where p_1 and p_2 satisfy a bilinear equation and q is determined by a nonlinear Riccati equation. With these stringent requirements, several specific solutions are presented to construct localized excitations. Through asymptotic analysis, we identified a resonant regime governing dromion-dromion/solitoff interactions, resulting in completely inelastic collisions. By employing a combination of symbolic computation techniques and the Hirota bilinear method, we derived specific solutions describing lump, lumpoff, and the resonant interaction between a lump and a line-soliton pair. Notably, the unique transient lump solution (42) possesses the essential features of a two-dimensional rogue wave mode, exhibiting localization in both the two-dimensional spatial domain and in time.

Acknowledgments

This work is supported by the National Natural Science Foundation of China (No. 12075208, No. 12275085 and No. 12235007) and Science and Technology Commission of Shanghai Municipality (No. 21JC1402500 and No. 22DZ2229014).

Data availability statement

No new data were created or analysed in this study.

Conflict of interest

All authors of this article declare no conflict of interest.

ORCID iDs

Jianyong Wang https://orcid.org/0000-0001-9583-5315
Yunqing Yang https://orcid.org/0000-0003-0576-6032
Xiaoyan Tang https://orcid.org/0000-0001-7180-3992
Yong Chen https://orcid.org/0000-0001-9230-5925

References

[1] Ablowitz M J and Clarkson P A 1991 *Soliton, Nonlinear Evolution Equations and Inverse Scattering* vol. 149 (Cambridge university press)
[2] Gardner C S, Greene J M, Kruskal M D and Miura R M 1976 Method for solving the Korteweg-deVries equation *Phys. Rev. Lett.* **19** 1095
[3] Rogers C and Schief W K 2012 *Bäcklund and Darboux transformations: geometry and modern applications in soliton theory* vol. 30 (Cambridge University Press)
[4] Li J B, Yang Y Q and Sun W Y 2024 Breather wave solutions on the Weierstrass elliptic periodic background for the (2+1)-dimensional generalized variable-coefficient KdV equation *Chaos* **34** 023141
[5] Hirota R 1971 Exact solution of the Korteweg-de Vries equation for multiple collisions of solitons *Phys. Rev. Lett.* **27** 1192
[6] Xu J and Fan E G 2015 Long-time asymptotics for the Fokas-Lenells equation with decaying initial value problem: Without solitons *J. Differ. Equ.* **259** 1098–148
[7] Zhao P and Fan E G 2020 Finite gap integration of the derivative nonlinear Schrödinger equation: a Riemann-Hilbert method *Physica* D **402** 132213
[8] Tian S F 2017 Initial-boundary value problems for the general coupled nonlinear Schrödinger equation on the interval via the Fokas method *J. Differ. Equ.* **262** 506–58
[9] Dai C Q, Wang Y Y, Tian Q and Zhang J F 2012 The management and containment of self-similar rogue waves in the inhomogeneous nonlinear Schrödinger equation *Ann. Phys.* **327** 512–21
[10] Cao C W 1990 Nonlinearization of the Lax system for AKNS hierarchy *Sci. China Ser.* A **33** 528–36
[11] Cheng Y and Li Y S 1991 The constraint of the Kadomtsev-Petviashvili equation and its special solutions *Phys. Lett.* A **175** 22
[12] Lou S Y and Ruan H Y 2001 Revisitation of the localized excitations of the (2+1)-dimensional KdV equation *J. Phys.* A **34** 305
[13] Tang X Y, Lou S Y and Zhang Y 2002 Localized excitations in (2+1)-dimensional systems *Phys. Rev.* E **66** 046601
[14] Tang X Y and Lou S Y 2003 Extended multilinear variable separation approach and multivalued localized excitations for some (2+1)-dimensional integrable systems *J. Math. Phys.* **44** 4000–25
[15] Lou S Y 2002 Dromions, Dromion lattice, breathers and instantons of the Davey-Stewartson equation *Phys. Scr.* **65** 7
[16] Tang X Y, Chen C L and Lou S Y 2002 Localized solutions with chaotic and fractal behaviours in a (2+1)-dimensional dispersive long-wave system *J. Phys.* A **35** L293
[17] Lou S Y 2002 (2+1)-dimensional compacton solutions with and without completely elastic interaction properties *J. Phys.* A **35** 10619
[18] Lou S Y 2003 Localized excitations of the (2+1)-dimensional sine-Gordon system *J. Phys.* A **36** 3877–92
[19] Tang X Y and Lou S Y 2002 A variable separation approach to solve the integrable and nonintegrable models: coherent structures of the (2+1)-dimensional KdV equation *Commun. Theor. Phys.* **38** 1
[20] Dai C Q and Zhang J F 2006 Novel variable separation solutions and exotic localized excitations via the ETM in nonlinear soliton systems *J. Math. Phys.* **47** 043501
[21] Cui C J, Tang X Y and Cui Y J 2020 New variable separation solutions and wave interactions for the (3+1)-dimensional Boiti-Leon-Manna-Pempinelli equation *Appl. Math. Lett.* **102** 106109
[22] Manakov S V, Zakhorov V E and Bordag L A 1977 Two-dimensional solitons of the Kadomtsev-Petviashvili equation and their interaction *Phys. Lett.* A **63** 205–6
[23] Ma W X 2015 Lump solutions to the Kadomtsev-Petviashvili equation *Phys. Lett.* A **379** 1975–8
[24] Ma W X and Zhou Y 2018 Lump solutions to nonlinear partial differential equations via Hirota bilinear forms *J. Differ. Equ.* **264** 2633–59
[25] Zhang H Q and Ma W X 2017 Lump solutions to the (2+1)-dimensional Sawada-Kotera equation *Nonlinear Dyn.* **87** 2305–10

[26] Abdeljabbar A, Hossen M B, Roshid H O and Aldurayhim A 2022 Interactions of rogue and solitary wave solutions to the (2+1)-D generalized Camassa-Holm-KP equation *Nonlinear Dyn.* **110** 3671–83
[27] Wazwaz A M 2023 Painlevé integrability and lump solutions for two extended (3+1)-and (2+1)-dimensional Kadomtsev-Petviashvili equations *Nonlinear Dyn.* **111** 3623–32
[28] Sun Y and Li B 2023 Creation of anomalously interacting lumps by degeneration of lump chains in the BKP equation *Nonlinear Dyn.* **111** 19297–313
[29] Hossen M B, Roshid H O, Ali M Z and Rezazadeh H 2021 Novel dynamical behaviors of interaction solutions of the (3+1)-dimensional generalized B-type Kadomtsev-Petviashvili model *Phys. Scr.* **96** 125236
[30] Li W and Li B 2024 Construction of degenerate lump solutions for (2+1)-dimensional Yu-Toda-Sasa-Fukuyama equation *Chaos Solitons Fract.* **180** 114572
[31] Guo F and Lin J 2019 Interaction solutions between lump and stripe soliton to the (2+1)-dimensional Date-Jimbo-Kashiwara-Miwa equation *Nonlinear Dyn.* **96** 1233–41
[32] Peng W Q, Tian S F and Zhang T T 2018 Analysis on lump, lumpoff and rogue waves with predictability to the (2+1)-dimensional B-type Kadomtsev-Petviashvili equation *Phys. Lett.* A **382** 2701–8
[33] Wang J Y, Yang Y Q, Tang X Y and Chen Y 2024 A novel (2+1)-dimensional Sawada-Kotera type system: multisoliton solution and variable separation solution *Nonlinear Dyn.* **112** 8481–94
[34] Sawada K and Kotera T 1974 A method for finding N-soliton solutions of the KdV equation and KdV-like equation *Prog. Theoret. Phys.* **51** 1355–67
[35] Caudrey P J, Dodd R K and Gibbon J D 1976 A new hierarchy of Korteweg-de Vries equations *Proc. R. Soc. London* A **351** 407–22
[36] Wang X B, Zhao Q, Jia M and Lou S Y 2022 Novel travelling wave structures for (2+1)-dimensional Sawada-Kotera equation *Appl. Math. Lett.* **124** 107638
[37] Baqer S and Smyth N F 2023 Whitham shocks and resonant dispersive shock waves governed by the higher order Korteweg-de Vries equation *Proc. R. Soc.* A **479** 20220580
[38] Ruan H Y and Chen Y X 2005 The role of the seed solution in solving nonlinear equations *Phys. Scr.* **72** 320
[39] Hirota R 2004 *The Direct Method in Soliton Theory (No.155)* (Cambridge University Press)
[40] Quan J F and Tang X Y 2023 New variable separation solutions and localized waves for (2+1)-dimensional nonlinear systems by a full variable separation approach *Phys. Scr.* **98** 125269
[41] Tang X Y, Cui C J, Liang Z F and Ding W 2021 Novel soliton molecules and wave interactions for a (3+1)-dimensional nonlinear evolution equation *Nonlinear Dyn.* **105** 2549–57
[42] Radha R, Singh S, Kumar C S and Lou S Y 2022 Elusive exotic structures and their collisional dynamics in (2+1)-dimensional Boiti-Leon-Pempinelli equation *Phys. Scr.* **97** 125211
[43] Singh K, McKerr M and Kourakis I 2023 Dust ion-acoustic dromions in Saturn's magnetosphere *Mon. Not. R. Astron. Soc.* **521** 2119–33
[44] Shi Z Y and Huang G X 2023 Matter-wave dromions in a disk-shaped dipolar Bose-Einstein condensate with the Lee-Huang-Yang correction *Phys. Rev.* E **107** 024214
[45] Martínez Alonso L and Medina Reus E 1992 Localized coherent structures of the Davey-Stewartson equation in the bilinear formalism *J. Math. Phys.* **33** 2947–57
[46] Lou S Y and Lin J 2018 Rogue waves in nonintegrable KdV-type systems *Chin. Phys. Lett.* **35** 050202